

INVESTIGATION OF OPTICAL CONSTANTS AND OPTICAL BAND GAP FOR AMORPHOUS $\text{Se}_{40-x}\text{Te}_{60}\text{Ag}_x$ THIN FILMS

S. SINGH, S. KUMAR*

Department of Physics, OPJS University, Churu, Rajasthan 331303 India

This paper reports the effect of silver (Ag) content on optical properties of amorphous chalcogenide glasses $\text{Se}_{40-x}\text{Te}_{60}\text{Ag}_x$ ($x = 0, 2, 4, 6, 8$). Thin films of $\text{a-Se}_{40-x}\text{Te}_{60}\text{Ag}_x$ glassy alloys have been synthesized by thermal evaporation technique under high vacuum conditions ($\sim 10^{-5}$ torr). The optical spectra of amorphous $\text{Se}_{40-x}\text{Te}_{60}\text{Ag}_x$ ($x = 0, 2, 4, 6, 8$) thin films have been measured by a double beam UV-VIS-NIR computer controlled spectrophotometer in the wavelength range 200-3000 nm. Swanepole technique has been used to calculate the optical constants [refractive index (n), extinction coefficient (k), real dielectric constant (ϵ'), imaginary dielectric constant (ϵ'') and absorption coefficient (α)] and optical band gap of amorphous $\text{Se}_{40-x}\text{Te}_{60}\text{Ag}_x$ thin films. Absorption coefficient (α) increases with incident photon energy ($h\nu$) for all the samples. The optical band gap increases with increase of the silver (Ag) content. The increase in optical band gap with increase of the Ag content has been explained on the basis of Mott and Davis Model.

(Received February 8, 2017; Accepted April 20, 2017)

Keywords: Thin films, Chalcogenide glasses, Defect states, Optical constants, Optical band gap etc.

1. Introduction

Chalcogenide glasses are oxygen-free inorganic glasses containing one or more chalcogen elements [1-2]. These glasses are formed by the addition of other elements such as Ag, As, Ge etc. Chalcogenide glasses are low-phonon-energy materials and are generally transparent from the visible to infrared region. These glasses based on sulfides, selenide and telluride alloys in binary and multi-component systems have evoked much interest in terms of the understanding of basic physics and its applications in semiconducting devices. These glasses have vast electrical, optical and technological applications, such as irreversible phase change optical recording, memory devices, optical fibers, xerography, photolithography, infrared lenses, optical amplifiers, blue laser diodes and in solar cells [3-12]. Chalcogenide glasses are known to have flexible structure, in the sense that each atom can adjust its neighboring environment to satisfy the valance requirements. Chalcogenide glasses are sensitive to the absorption of electromagnetic radiation and show a variety of photo-induced effects and various models have been put forward to explain these effects, which can be used to fabricate diffractive, wave-guide and fiber structures [13-14]. As chalcogenide glasses have poor thermo-mechanical properties, in order to enlarge their domain of applications, it is necessary to increase their softening temperature and mechanical strength. The interest in these materials arises particularly due to their ease of fabrication in the form of bulk and thin films.

The addition of tellurium (Te) has a catalytic effect on the crystallization of selenium. The presence of Te in Se chains probably favors their thermal dissociation as the Se-Te bond being weaker than Se-Se bond [15]. Se-Te alloys have created extreme interest due to their greater hardness, higher photosensitivity, higher crystallization temperature and lower aging effects as compared to pure amorphous Se [16-17]. The addition of Se into Te improves the corrosion resistance [18]. Therefore, Se-Te based alloys are thought to be a good promising media, which make use of a phase change between an amorphous state and a crystalline state.

The effect of an impurity in an amorphous semiconductor material may be widely different, depending on the conduction mechanism and the structure of material [19]. The impurity

may either destroy the dangling bond centres of one sign or form charged centres which are compensated by centers of opposite sign. In the present study work Ag has been chosen as an additive element in Se-Te alloys. The third element behaves as chemical modifier as it is reported to expand the glass forming region. The addition of third element like Ag in Se-Te binary alloy is expected to change the optical and electrical properties of host alloy. A typical chalcogenide has a relatively sharp optical absorption edge, single electrical activation energy, efficient photo excited conductivity and luminescence. The study of the optical properties of chalcogenide glasses is important for the determination of the electronic band structure as well as other optical parameters, such as optical energy gap and refractive index. The aim of present paper is to study the effect of Ag incorporation on the optical properties of Se-Te alloys. The optical transmission spectra of the amorphous thin films of $a\text{-Se}_{40-x}\text{Te}_{60}\text{Ag}_x$ are measured by spectrophotometer. Optical parameters like refractive index, extinction coefficient, real and imaginary dielectric constants, absorption coefficient and optical band gap have been calculated for a $\text{Se}_{40-x}\text{Te}_{60}\text{Ag}_x$ glassy system.

2. Experimental Procedure

Glassy alloys of $a\text{-Se}_{40-x}\text{Te}_{60}\text{Ag}_x$ ($x = 0, 2, 4, 6, 8$) were prepared by melt-quenching technique. High purity 99.999% Se, Ag and Te granules were weighted according to the formula of $a\text{-Se}_{40-x}\text{Te}_{60}\text{Ag}_x$ ($x = 0, 2, 4, 6, 8$). The powder mixture was loaded into quartz ampoule and sealed under vacuum at 10^{-5} torr. The sealed quartz ampoules was loaded in a furnace and heated to 950°C at a rate of $3\text{-}4^\circ\text{C}/\text{minute}$ for 18 hours to ensure the composition homogeneity and quenched in liquid nitrogen. The ingots were crushed, separated, grounded and characterized. The glassy nature of alloys was checked with the help of X-ray diffraction technique using Cu-K α radiation.

The thin films of chalcogenide were synthesized by thermal evaporation technique under high vacuum conditions ($\sim 10^{-5}$ torr) using a small piece of bulk alloy as a source material and glass as a substrate. The films were kept inside the deposition chamber for 24 hours to achieve the metastable equilibrium. The optical transmission spectra of amorphous $\text{Se}_{40-x}\text{Te}_{60}\text{Ag}_x$ ($x = 0, 2, 4, 6, 8$) thin films have been measured by a double beam UV-VIS-NIR computer controlled spectrophotometer as a function of wavelength.

3. Result and Discussion

Optical transmission coefficient (T) is a very complex function and found to be dependent on the absorption coefficient (α). The variation of optical transmission coefficient (T) with wavelength (λ) for amorphous $\text{Se}_{40-x}\text{Te}_{60}\text{Ag}_x$ thin films is shown in Fig. 1.

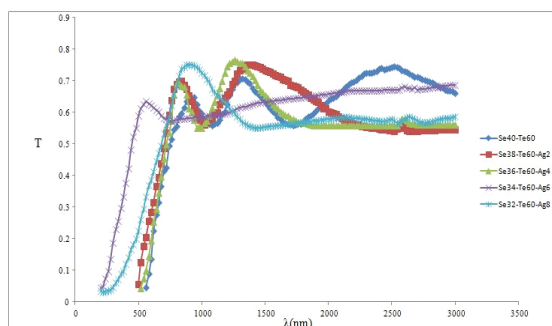


Fig. 1 Variation of optical transmittance (T) with wavelength (λ) for amorphous $\text{Se}_{40-x}\text{Te}_{60}\text{Ag}_x$ thin films

Fig. 1. Variation of optical transmittance (T) with wavelength (λ) for amorphous $\text{Se}_{40-x}\text{Te}_{60}\text{Ag}_x$ thin films

By the well known Swanepole's method [20], which is based on Mainfacer theory [21], the envelope of the interference maxima and minima occurs in the spectrum and the presence of these maxima and minima position confirmed the optical homogeneity of the deposited film and no scattering and absorption occurs at long wavelengths. This technique has been used by various researchers in chalcogenide glasses [22-23].

3.1 Determination of Optical Constants

By Swanepole's method [20], the optical parameters are deduced from the fringe patterns in the transmittance spectrum. In the transmittance region where the absorption coefficient ($\alpha = 0$), the refractive index n is given by

$$n = [N + (N^2 - s^2)^{1/2}]^{1/2} \quad (1)$$

where $N = (2s / T_m) - (s^2 + 1) / 2$, s is the refractive index of the substrate and T_m is the envelope function of the transmittance minima.

Where ($\alpha \neq 0$), in the region of weak and medium absorption, the refractive index n is given by

$$n = [N + (N^2 - s^2)^{1/2}]^{1/2} \quad (2)$$

where $N = \{2s(T_M - T_m) / T_M T_m + (s^2 + 1) / 2$ and T_m is the envelope function of the transmittance maxima.

In the region of strong absorption, the transmittance decreases drastically and refractive index (n) can be estimated by extrapolating the values in the other regions.

If n_1 and n_2 are the refractive indices at two adjacent maxima and minima at λ_1 and λ_2 then the thickness of the film (d) is given by

$$d = \lambda_1 \lambda_2 / 2[\lambda_1 n_2 - \lambda_2 n_1] \quad (3)$$

The extinction coefficient (k) can be calculated by relation

$$k = \alpha \lambda / (4\pi) = (\lambda / 4\pi d) \ln (1/x) \quad (4)$$

where x is the absorbance and d is the film thickness.

In the region of weak and medium absorption, absorbance (x) can be calculated from the transmission minima T_m and given in equation (5)

$$x = [E_m - \{E_m - (n^2 - 1)^3 (n^2 - s^4)^{1/2}\} / [(n - 1)^3 (n - s^2)]] \quad (5)$$

where $E_m = [(8n^2/s/T_m) - (n^2 - 1)(n^2 - s^2)]$

The obtained values of refractive index and extinction coefficient are given in Table 1. The variation of refractive index with photon energy ($h\nu$) is shown in Fig. 2 and the variation of extinction coefficient with photon energy is shown in Fig. 3. It is observed that the value of refractive index and extinction coefficient show an overall increasing trend with the increase in photonic energy. From Table 1, it is observed that the values of refractive index (n) and extinction coefficient (k) increases with the increase of Ag content for a-Se_{40-x}Te₆₀Ag_x thin films. This spectral and dopant dependence of optical constants with the photonic energy will be helpful in deciding on the suitability of this system for application in optical data storage devices. The real and imaginary part of the dielectric constant of amorphous thin films has been calculated by the relation (6) and (7), respectively

$$\epsilon' = n^2 - k^2 \quad (6)$$

$$\epsilon'' = 2nk \quad (7)$$

The variation of real and imaginary parts of the dielectric constant with photon energy is presented in Figs. 4 and 5 respectively. The calculated values of real part and imaginary part of the dielectric constant are also presented in Table 1. These are found to increase with the increase in photon energy and also with addition of Ag impurity in the present system of $a\text{-Se}_{40-x}\text{Te}_{60}\text{Ag}_x$ thin films.

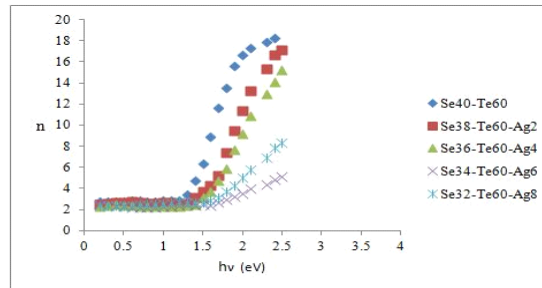


Fig 2. Variation of refractive index (n) with photon energy ($h\nu$) for amorphous $\text{Se}_{40-x}\text{Te}_{60}\text{Ag}_x$ thin films

Fig. 2. Variation of refractive index (n) with photon energy ($h\nu$) for amorphous $\text{Se}_{40-x}\text{Te}_{60}\text{Ag}_x$ thin films

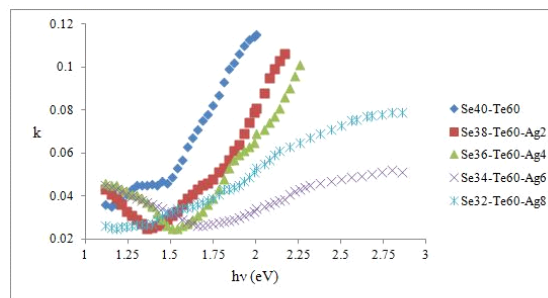


Fig 3. Variation of extinction coefficient (k) with photon energy ($h\nu$) for amorphous $\text{Se}_{40-x}\text{Te}_{60}\text{Ag}_x$ thin films.

Fig. 3. Variation of extinction coefficient (k) with photon energy ($h\nu$) for amorphous $\text{Se}_{40-x}\text{Te}_{60}\text{Ag}_x$ thin films

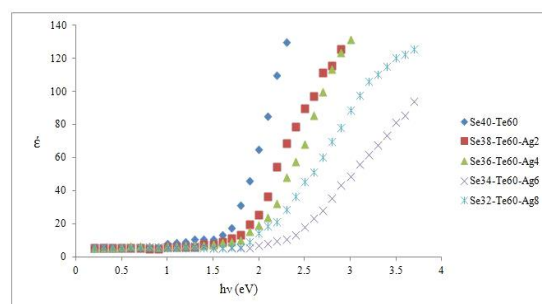


Fig 4. Variation of real dielectric constant (ϵ') with photon energy ($h\nu$) for amorphous $\text{Se}_{40-x}\text{Te}_{60}\text{Ag}_x$ thin films

Fig. 4. Variation of real dielectric constant (ϵ') with photon energy ($h\nu$) for amorphous $\text{Se}_{40-x}\text{Te}_{60}\text{Ag}_x$ thin films

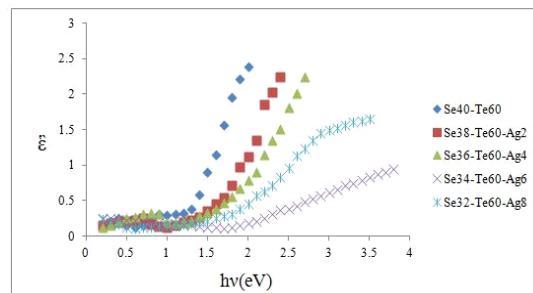


Fig 5. Variation of imaginary dielectric constant with photon energy ($h\nu$) for amorphous $Se_{40-x}Te_{60}Ag_x$ thin films.

Fig. 5. Variation of imaginary dielectric constant with photon energy ($h\nu$) for amorphous $Se_{40-x}Te_{60}Ag_x$ thin films

3.2 Absorption Coefficient and Optical Band Gap

The absorption coefficient (α) of amorphous $Se_{40-x}Te_{60}Ag_x$ thin films have been calculated by using relation (8)

$$\alpha = 4\pi k / \lambda \quad (8)$$

Here an increase in the value of absorption coefficient (α) with the increase in photon energy for a- $Se_{40-x}Te_{60}Ag_x$ thin films and it is also observed that the value of absorption coefficient increases with the increase of Ag content. Due to the large absorption coefficient these materials may be suitable for optical memory storage devices.

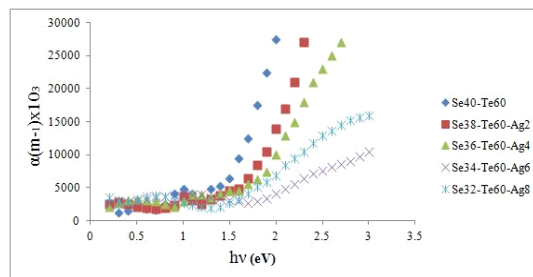


Fig 6. Variation of absorption coefficient (α) with photon energy ($h\nu$) for amorphous $Se_{40-x}Te_{60}Ag_x$ thin films.

Fig. 6. Variation of absorption coefficient (α) with photon energy ($h\nu$) for amorphous $Se_{40-x}Te_{60}Ag_x$ thin films

The optical band gap is calculated from absorption coefficient data as a function of energy ($h\nu$) by using Tauc relation [24-25].

$$\alpha = A(h\nu - E_g)^n / h\nu \quad (9)$$

Here A is a constant, E_g is the optical band gap of the material and the exponent n depends on the type of transition and have values 1/2, 2, 3/2 and 3 corresponding to the allowed direct, allowed indirect, forbidden direct and forbidden indirect transitions, respectively.

The present system of a- $Se_{40-x}Te_{60}Ag_x$ obeys the rule of allowed indirect transition. The values of optical band gap (E_g) is calculated by extrapolating the straight line portion of $(\alpha h\nu)^{1/n}$ vs. $h\nu$ by taking $n = 2$ as shown in Fig. 7. The calculated values of E_g for all samples are given in Table 1. It is evident from Table 1, that the optical band gap (E_g) increases with increase of the Ag content. The increase in optical band gap with increase of the Ag content can be explained on the basis of Mott and Davis Model [24]. According to this technique, chalcogenide thin films contain a

high concentration of defect states and these defects are responsible for the presence of localized states in the band gap. The variation of optical band gap with silver concentration is shown in Fig. 8. The increase in optical band gap with increase of the Ag content may be due to decrease in the density of defect states in the mobility gap or increase in disorderness. The increase in optical band gap along with the decrease in the density of defect states may also be correlated with electronegativity of the elements involved. The electronegativity of Se, Te and Ag are 2.4, 2.1 and 1.93 respectively and Ag has lower electronegativity than Se. The valance band of chalcogenide glasses contains the loan pair p-orbital and addition of electropositive element (Ag) to electronegative element (Se) may raise the energy of loan pair states, which is further responsible for the broadening of the valance band inside the forbidden gap and leads to band tailing and hence band gap expanding.

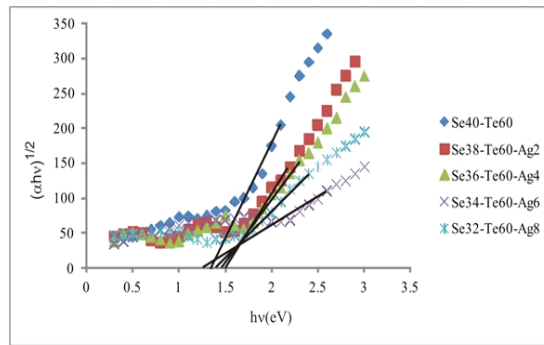


Fig. 7. Variation of $(\alpha hv)^{1/2}$ with photon energy (hv) for amorphous $Se_{40-x}Te_{60}Ag_x$ thin films

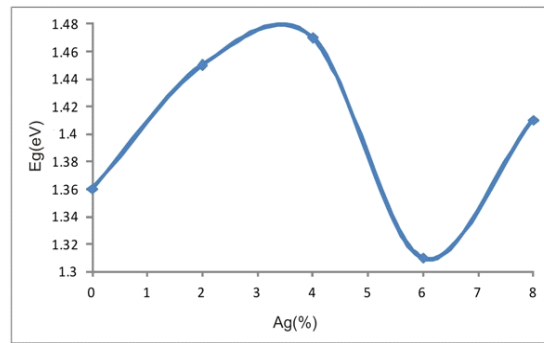


Fig. 8. Variation of optical band gap (E_g) with silver (Ag) concentration for amorphous $Se_{40-x}Te_{60}Ag_x$ thin films

Table 1: Optical parameters for amorphous $Se_{40-x}Te_{60}Ag_x$ thin films at 1600 nm.

Material	Refractive Index (n)	Extinction Coefficient(k)	Real Dielectric Constant (ϵ')	Imaginary Dielectric Constants (ϵ'')	Absorption Coefficient (α)(m^{-1}) $\times 10^3$	Optical Band Gap E_g (eV)
Se40Te60	16.65	0.115	65.00	2.39	27.50	1.36
Se38Te60Ag2	11.35	0.081	25.25	1.12	14.00	1.45
Se36Te60Ag4	9.15	0.069	19.33	0.79	10.10	1.47
Se34Te60Ag6	3.55	0.034	7.23	0.18	4.10	1.31
Se32Te60Ag8	5.05	0.053	14.15	0.46	6.90	1.41

These indirect band gap materials may have potential applications in optical recording media, infrared spectroscopy, laser fibers, xerography, fiber optical telecommunication and electrographic applications. Moreover, their refractive index and transparency in the infrared region are good indicators for integrated optics and detection in the near-infrared spectral domain.

4. Conclusions

Thin films of a- $\text{Se}_{40-x}\text{Te}_{60}\text{Ag}_x$ glassy alloys have been synthesized by thermal evaporation technique by using amorphous bulk alloy as a source material and glass as a substrate under high vacuum conditions ($\sim 10^{-5}$ torr). The optical transmission spectra of amorphous $\text{Se}_{40-x}\text{Te}_{60}\text{Ag}_x$ ($x = 0, 2, 4, 6, 8$) thin films have been measured by a double beam UV-VIS-NIR computer controlled spectrophotometer. Swanepole method has been used to calculate the refractive index, real and imaginary dielectric constants, extinction coefficient, absorption coefficient and optical band gap.

The refractive index (n), extinction coefficient (k), real dielectric constant (ϵ'), imaginary dielectric constant (ϵ'') and absorption coefficient (α) increase with increase of photon energy and decrease with increase of Ag concentration up to $x = 0, 2, 4$ and 6% and increase all the calculated optical parameters are increase for Ag at $x = 8\%$. The optical band gap (E_g) increases with increase of the Ag content.

The increase in optical band gap with increase of the Ag content may be due to decrease in the density of defect states in the mobility gap or increase in disorderness and reverse order may be possible for a particular concentration of $x = 8\%$ in the study sample, but at $x = 6\%$ of Ag content, the minimum values of optical band gap and other optical parameters due to may be increase the density of defect states or decrease the the disorderness in the mobility gap for this concentration of Ag. On the basis of above calculated values of optical parameters, one may decide the suitability of these materials for optical storage devices.

References

- [1] J. S. Sanghera, J. Heo, J. D. Mackenzie, *J. Non-Cryst. Solids* **103**, 155 (1988).
- [2] V. Pandey, S.K. Tripathi, A. Kumar, *Journal of Ovonic Research* **2**, 67 (2006).
- [3] M. Saxena, S. Gupta, A. Agarwal, *Adv. Appl. Sci. Research* **2**(2), 109 (2011).
- [4] G. Kaur, T. Komatsu, *J. Mater. Sci.* **36**, 453 (2001).
- [5] Z. Abdel-Khalek Ali, G.H. Adel, A.S. Abd-rbo, *Chalc. Lett.* **6**, 125 (2009).
- [6] V. Trnovcova, I. Furar, D. lezal, *J. Non-Cryst. Solids* **353**, 1311 (2007).
- [7] A. Kumar, P. B. Barman, R. Sharma, *Adv. Appl. Sci. Research* **1**(2), 47 (2010).
- [8] A. Kumar, M. Lal, K. Sharma, S. K. Tripathi, N. Goyal, *Chalc. Lett.* **9**, 275 (2012).
- [9] V. K. Saraswat, V. Kishore, K. Singh, N. S. Sexana, T. P. Sharma, *Chalc. Lett.* **3**, 61 (2006).
- [10] R. M. Mehra, G. Kaur, P. C. Mathur, *J. Mater. Sci.* **26**, 3433 (1991).
- [11] A. A. Manshina, A. V. Kurochkin, S. V. Degtyarev, Ya. G. Grigoriev, A. S. Tverjanovich, Yu. S. Tveryanovich, V. B. Smirnov, *Proc. SPIE* **4429**, 80 (2001).
- [12] A. S. Tverjanovich, Ya. G. Grigoriev, S. V. Degtyarev, A. V. Kurochkin, A. A. Manshina, Yu. S. Tveryanovich, *J. Non-Cryst. Solids* **286**, 89 (2001).
- [13] A. B. Seddon, *J. Non-cryst. Solids* **44**, 184 (1995).
- [14] J. S. Sanghera, I. D. Agrwal, *J. Non-cryst. Solids* **6**, 256 (1999).
- [15] M. Saxena, *J. Physics D: Applied Physics* **38**, 460 (2005).
- [16] R. K. Shukla, S. Swarup, A. Kumar, A. N. Nigam, *Phys. Stat. Sol. (a)* **K 105**, 115 (1989).
- [17] H. Yang, W. Wang, S. Min, *J. Non-cryst. Solids* **80**, 503 (1986).
- [18] R. Chiba, N. Funakoshi, *J. Non-cryst. Solids* **105**, 149 (1988).
- [19] N. F. Mott, *Philos. Mag.* **19**, 835 (1969).
- [20] R. Swanepoel, *J. Phys. E.* **16**, (1983) 1214.
- [21] J. C. Manificier, J. Gasiot, J. P. Fillard, *J. Phys. E. Sci. Instrum.* **9**, 1002 (1976).
- [22] S. M. Ei-Sayed, *Vacuum* **72**, 169 (2004).

[23] H. S. Metcoally, *Vaccum* **62**, 345 (2001).

[24] N. F. Mott, E. A. Davis, *Electronic Processes in Non-Crystalline Mat.*, Clarendon, Oxford, 1979, 428.

[25] M. M. Wakkad, E. Kh. Shoker, S. H. Mohamed, *J. Non-Cryst. Solids* **157**, 265 (2000).